A Vibration-Free 35 K Cryocooler Driven by Electrochemical Compressors

W. Chen, B. Smith, M. Zagarola, S. Narayanan[1]

Creare Incorporated
Hanover, NH 03755

[1]Loker Hydrocarbon Research Institute, University of Southern California
Los Angeles, CA 90089

ABSTRACT

This paper reports on the development of a vibration-free cryocooler for infrared detectors for surveillance and missile tracking. The cryocooler employs a solid-state Electro-Chemical Hydrogen Compressor (ECHC) for vibration-free operation. A unique single-pressure dilution cycle was developed that enables an upper stage driven by an ECHC to provide precooling for the lower hydrogen Joule-Thomson (J-T) stage. The ECHC uses an advanced anhydrous proton conducting membrane to compress hydrogen through an electro-chemical process. This compressor produces high pressure ratios with no moving parts. Proof-of-concept anhydrous proton conductive membranes were fabricated, and their performances were characterized in a test cell. Based on the membrane performance data, the thermodynamic cycle design of the cryocooler was optimized and then the cryocooler performance was estimated. Preliminary mechanical designs for the ECHCs were also developed.

INTRODUCTION

Cryocoolers that use mechanical compressors, especially those operating at low frequencies (< 1000 Hz), can produce significant vibrations on spacecraft, which can cause substantial image artifacts. Some mechanical compressors also have limited reliability due to mechanical fatigue or wear. Solid-state cryocoolers with no moving parts are highly desirable because they enhance system reliability and produce no jitter.

Current research in the area of solid-state cryocoolers focuses mainly on magnetic coolers, thermoelectric coolers (TEC), and optical coolers. So far, however, the ability of these cooling technologies to provide active cooling at 35 K with a 300 K heat sink has not been demonstrated. In a magnetic cooler, the local temperature swing associated with the magnetization and demagnetization processes is still limited to only a few Kelvin, even with a very strong field swing (>3 T). Multiple stages are needed to achieve an adequate temperature difference. Optical coolers require extremely pure materials for the cooling element, since the heat generated in the contaminants (due to nonradioactive transitions) can overwhelm the fluorescent cooling. In solid materials (as opposed to atomic gases), the anti-Stokes fluorescent cooling effect decreases with temperature. Demonstration of fluorescent cooling in solid materials at temperatures below 50 K has not been reported. For TECs, the electrical resistivity and the

Cryocoolers 17, edited by S.D. Miller and R.G. Ross, Jr.

thermal conductivity of existing TEC materials are still too high, resulting in large internal joule heating and large conductive heat leak from the hot side to the cold side of a TEC. This severely limits a TEC's efficiency and its maximum temperature difference. Cooling temperatures below 150 K have not been demonstrated by a TEC.

Because of these limitations in current solid-state cryocooler technologies, there is a strong need for alternative technologies to achieve efficient cooling to temperatures below 35 K while rejecting heat at significantly higher temperatures.

A Solid-State Cryocooler with Electrochemical Compressors

An efficient cryocooler driven by solid-state ECHCs is being developed to provide cooling at temperatures below 35 K and reject heat at temperatures above 300 K. The operations of the ECHC and the cryocooler are discussed in detail below.

ECHC Concept Description. In an ECHC, low-pressure hydrogen is first ionized at the anode by removing its electrons. The resulting protons are then pulled across the membrane through a voltage potential. Finally, the protons are recombined with electrons at the cathode to form high-pressure hydrogen (Figure 1).

The most critical component in the ECHC is the proton conducting membrane. The membrane must have a high proton conductivity to minimize parasitic voltage drop across the membrane. The total cell voltage of an ECHC consists of the Nernst potential and the parasitic potentials, which include the total polarization voltage at the anode and cathode and the ohmic voltage drop (i.e., $I \times R_{mem}$). The Nernst potential ΔV_N depends on the ratio of the cathode pressure to the anode pressure and can be calculated by the following Nernst equation:

$$\Delta V_N = \frac{RT}{2F} \ln\left(\frac{p_c}{p_a}\right) \tag{1}$$

where ΔV_N is the Nernst potential, R is universal gas constant, T is the cell temperature, F is the Faraday constant, and p_c and p_a are the cathode and anode pressures. Typically, the polarization voltage is negligible and the cell total voltage ΔV_m is given by:

$$\Delta V_m = \Delta V_N + IR_{mem} \tag{2}$$

where I is the current passing though the membrane and R_{mem} is the membrane electrical resistance.

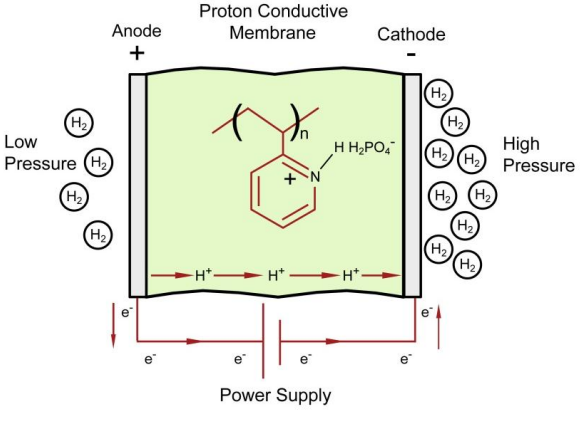

Figure 1. Operating mechanism of electrochemical hydrogen compressor

Reducing the membrane thickness or current density across the membrane will reduce parasitic potential and therefore improve the compressor efficiency, which can be expressed by:

$$\eta_{isothermal} = \frac{\Delta V_N I}{\Delta V_m I} = \frac{1}{1 + \dfrac{2FJ\delta}{RT\ln(p_c/p_a)\sigma}} \tag{3}$$

where J is the current density, δ is the membrane thickness, and σ is the membrane proton conductivity. Operating the membrane compressor at higher compression ratios (p_c/p_a) will increase the useful work output at constant parasitic loss, and will therefore also improve the compressor efficiency. These effects can be seen in Equation (3). In relative low-pressure operations (<100 bar), back diffusion of hydrogen gas from the high-pressure side to the low-pressure side is negligible.

For cryogenic applications, the hydrogen flowing out of the ECHC must be free of contamination. Water-free proton conducting membranes include three types: ceramic, ceramic/metal, and polymeric. Ceramic or ceramic/metal membranes must operate above 600 K to achieve acceptable conductivity. Polymer proton conductive membranes, on the other hand, have high enough conductivity in the 400 K range. Because compressing gas at very high temperatures is thermodynamically inefficient and requires a large recuperator to cool the gas to about 300 K, it is not practical to use a ceramic or ceramic/metal membrane for cryocooler applications. The lower operating temperatures make anhydrous polymeric membranes more suitable for cryocooler applications. Their operating temperatures are only about 100 K higher than the nominal heat rejection temperatures from spacecraft. The inefficiency associated with gas compression at these higher temperatures is within the acceptable range. Furthermore, operating the ECHC at this elevated temperature can reduce the size of the radiator that rejects the waste heat, and this helps reduce the overall vehicle mass.

Most current ECHCs use a hydrated Nafion® membrane as the proton conducting membrane. Proton conduction in such membrane materials relies on the presence of water. In these membranes, the proton is transported under a field by the Grotthus mechanism involving hopping and rapid rotation of water molecules, or by vehicular transport of hydronium ions. In the absence of water in anhydrous membranes, it is necessary to rely on other mechanisms for proton conductivity. Jet Propulsion Laboratory has developed new membranes that do not rely on water molecules for proton transport. These membranes operate on the ionization of polymeric acid-based salts and field-induced transport of protons; see Narayanan et al. [1]. Specifically, anhydrous high molecular weight polymeric organic amine salts have been prepared into membranes of the bisulfates and dihydrogen phosphates of poly-2-vinylpyridine (P2VP), poly-4-vinylpyridine (P4VP), and polyvinylimidazoline (PVI). These membranes have been found to have high proton conductivity in the temperature range of 25°C to 180°C. For this reason, this type of anhydrous membranes was evaluated for cryocooler applications.

Cryocooler Concept Description. The cycle schematic of the cryocooler incorporating the ECHC technology is shown in Figure 2. The upper stages of the proposed cryocooler utilize a unique dilution cycle that uses a gas with a strong J-T effect as the refrigerant and hydrogen gas as the diluent. The total gas pressures in the dilution cycle are nominally the same everywhere. Hydrogen is used to change the partial pressure of the refrigerant. The hydrogen partial pressure itself is controlled by an ECHC. On the anode side (low hydrogen partial pressure side) of the ECHC, hydrogen is pumped out of the hydrogen-refrigerant mixture as it flows from the inlet to the outlet. Consequently, the partial pressure of refrigerant gradually increases while the hydrogen partial pressure gradually decreases. This leads to a gradually increasing hydrogen pressure ratio across the membrane from the anode inlet to the outlet. The outlet pure hydrogen stream from the cathode side along with the refrigerant flow from the anode side are precooled by the returning stream to the ECHC; then they mix together at the cold end. During this mixing process, the partial pressure of the refrigerant is reduced significantly.

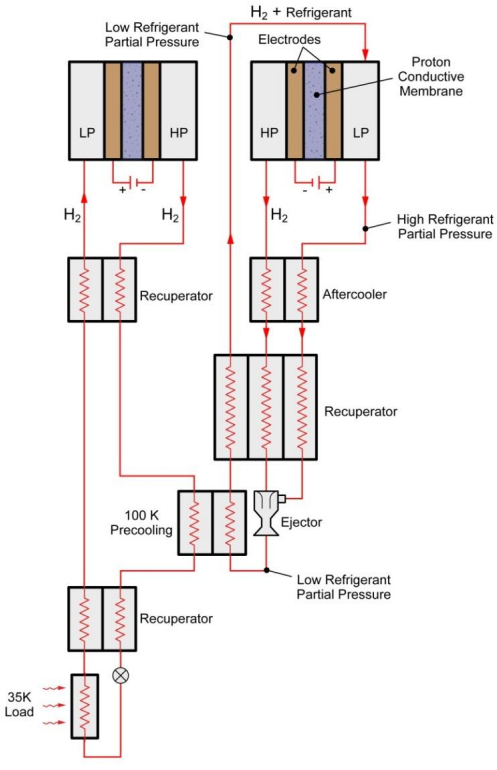

Figure 2. Cycle schematic of the solid-state cryocooler incorporating the ECHC technology

This is equivalent to a J-T expansion process for the refrigerant if the Van der Waals interaction between refrigerant and hydrogen molecules is small. In practice, more than one upper stage can be used to improve the system efficiency. Ejectors are used in the mixing process to allow the cathode hydrogen flow to raise the pressure of the refrigerant flow from the anode to overcome the pressure drops in the loop (Figure 2).

The lower stage of the cryocooler employs a conventional J-T cycle that uses hydrogen as the refrigerant to provide cooling for detectors at 35 K. Compression of the hydrogen gas is directly achieved by an ECHC. The temperature of hydrogen gas is precooled by the upper stage to temperatures significantly below its inversion temperature.

Anhydrous ECHC Fabrication and Testing

Several anhydrous poly-2-vinyl pyridinium dihydrogen phosphate salt membranes were fabricated at the University of Southern California, as shown in Figure 3. These membranes were used to assemble three membrane electrode assemblies (MEA), each with an active area of 5 cm2. Each MEA consisted of two platinum-catalyzed electrodes bonded to either side of the anhydrous PVP phosphate membrane. The MEA was mounted in an electrochemical test cell that consisted of two graphite plates with flow fields and ports for supply of reactants. The MEA was held between the graphite plates and gaskets. The cell is also equipped with heating pads on either side to allow it to operate at elevated temperature. A potentiostat/impedance analyzer was connected to the cell to make conductivity and polarization measurements. The detailed discussions about the fabrication processes and performance characterization of the membrane can be found in the paper by Yang, et al. [2]. The following sections briefly present technical aspects that are directly related to cryocooler applications.

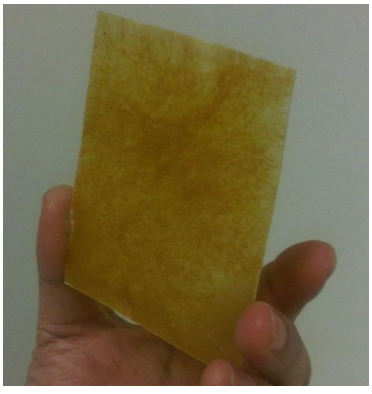

Figure 3. Anhydrous poly-2-vinyl pyridinium dihydrogen phosphate salt membrane fabricated at USC

Membrane Conductivity Measurement. Preliminary measurement of the conductivity of the membrane was carried out. The conductivity was calculated from the impedance measurements at 100 kHz. The conductivity rises with increasing temperature, as shown in Figure 4, indicating that ionic transport is responsible for the conductivity. The conductivity of the membrane shows Arrhenius type dependence and the activation energy was 50 kJ/mole. The specific ionic conductivity of the membrane at 140°C was 0.01 S cm^{-1}.

MEA Bakeout Testing. Prior to the bakeout test, a membrane sample was pretreated at 100°C for 72 hours. Then the membrane sample was kept at 120°C for over 48 hours. About 2.3% weight loss was observed after 24 hours of bakeout. The weight was stable thereafter, indicating that the initial weight loss was due to the dehydration of the membrane. The membrane did not show any sign of degradation after this testing. This result suggests that the anhydrous membrane can operate stably at the design temperature of about 120°C.

Hydrogen Pumping Experiments. Proof-of-concept hydrogen compression was demonstrated with the anhydrous membrane. A compression ratio higher than 3 was achieved with an atmospheric inlet pressure, as shown in Figure 5. At 140°C and a compression ratio of 1.5, the theoretical cell voltage is 0.0072 V. The actual steady-state voltage was 0.073 V at 2 mA/cm^2, corresponding to a compression efficiency of almost 10%; 95% of the inefficiency results from the resistance of the membrane. By using a membrane that is just 200 microns thick, the efficiency can be increased to about 30%. In these tests, the maximum compression ratio was limited by the pressure rating of the test cell, not by the membrane.

Proof-of-Concept Hydrogen Compressor Using Nafion Membrane. A proof-of-concept hydrogen compressor using a commercial hydrous Nafion membrane was also assembled and tested to calibrate the ECHC design model. A commercial MEA consisting of a 50 cm^2 Nafion membrane was used in the compressor. The thickness of the MEA is about 0.5 mm.

Test data show that it only takes a very small voltage, less than 0.1 V, across the MEA for the ECHC to develop a relatively large compression ratio of 3. The current density is on the order of 100 mA/cm^2. The measured resistance across the ECHC shows that the proton conductivity of the Nafion film itself is higher than 0.36 S/cm^2, agreeing well with the published data. The compressor net flow rates match very well with proton flow rates determined from electrical currents to electrodes. This suggests internal leakage or back diffusion is negligible. At low current density, the ECHC achieves very impressive isothermal compression efficiency higher than 30% (Figure 6), especially considering that the power input to the compressor is less than 1 W. The compression efficiency would be even higher at larger compression ratios because the parasitic losses do not increase appreciably with compression ratio while the useful work does.

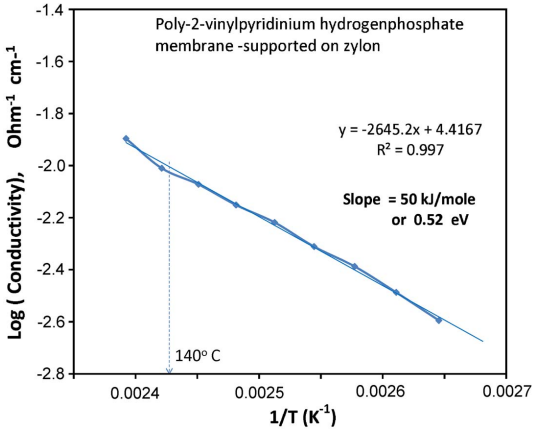

Figure 4. Ionic conductivity as a function of temperature for P2VP-DHP membrane

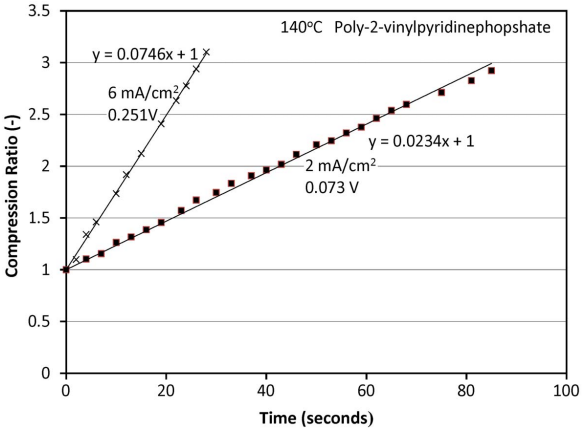

Figure 5. Compression of hydrogen at 140°C using P2VP-DHP membrane

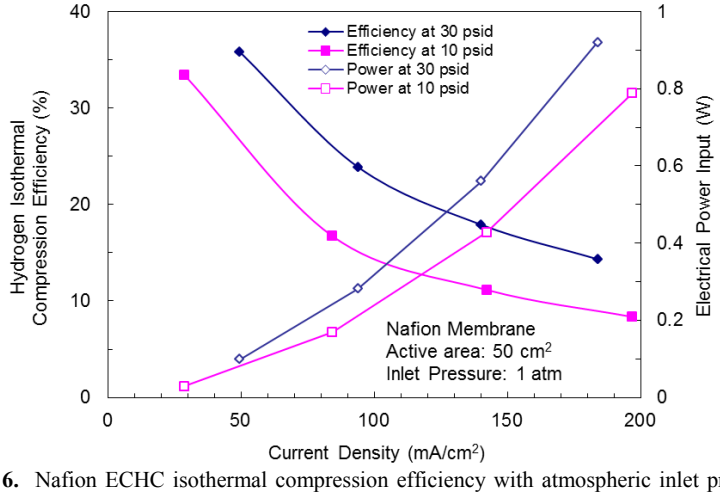

Figure 6. Nafion ECHC isothermal compression efficiency with atmospheric inlet pressure. The compressor achieves very competitive efficiency (above 30%) at high compression ratios.

Predicted ECHC Performance. Based on the proton conductivity of the anhydrous P2VP-DHP membrane and the operating characteristics of the proof-of-concept ECHCs, the predicted compression efficiency of a near-term ECHC with current anhydrous membranes is about 10 to 40% under representative operating conditions (Figure 7).

Integrated Cryocooler Design

Cycle Analysis and Optimization. The cycle configuration of a three-stage cryocooler was developed, and the cycle operating conditions were optimized to maximize its overall efficiency based on the performance characteristics of the anhydrous membrane. Key design parameters include the cooling temperatures for the first and second stages, as well as the refrigerant and hydrogen pressures in each stage. Several design considerations that are unique to this cryocooler are discussed below.

- The efficiency of an ECHC increases substantially as the compression ratio increases, as shown in Figure 7. Therefore, the pressure ratio in the ECHC for the hydrogen J-T stage should be relatively high for efficient operation. The maximum pressure on the high pressure in general is limited by the ECHC structural design consideration.
- The refrigerant compression ratio in a dilution cycle is controlled by the molar flow rate ratio of the hydrogen stream to the refrigerant stream before they are mixed together. Therefore, increasing the refrigerant pressure ratio will increase not only the hydrogen compression ratio in an ECHC, but also the hydrogen flow rate for a given refrigerant flow rate. This can lead to a much higher power input for the ECHC, even though the high pressure ratio will enhance the specific cooling power of the refrigerant flow.
- The hydrogen pressure ratio across an ECHC in a dilution cycle is not a constant value. On the anode side of an ECHC, the local hydrogen partial pressure gradually decreases along the flow direction as hydrogen is forced through the membrane. This effect needs to be taken into account in estimating the efficiency of an ECHC.

The key cycle operating parameters and predicted performance for the 35 K cryocooler are summarized in Table 1. For this particular design, the optimum cooling temperatures for the first and second stages are at 180 K and 100 K, respectively. The cooling loads for these two upper stages are both about 0.2 W, similar to the target cooling power of 0.2 W at the third stage. The maximum pressure in the cryocooler is 70 bar.

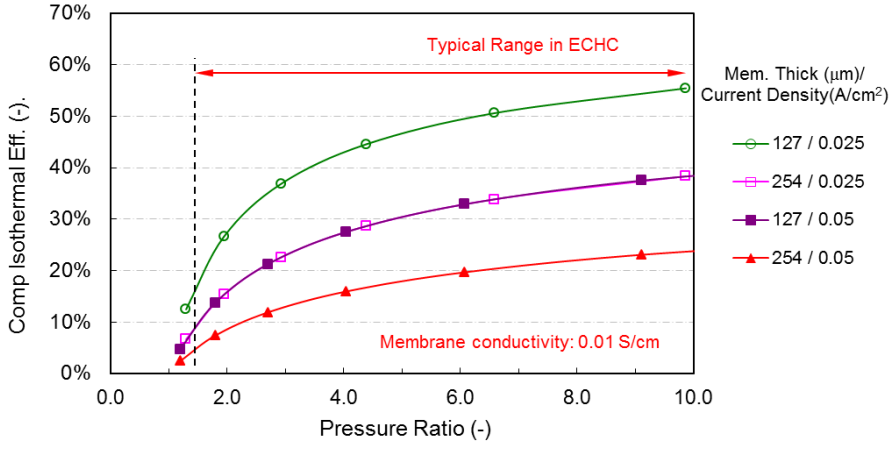

Figure 7. The predicted isothermal compression efficiency of a near-term ECHC as a function of compression ratio, membrane thickness, and current density

Table 1. Operating conditions and predicted performance for a 0.2 W cryocooler at 35 K

	Upper Stage		3rd H_2 J-T Stage
	1st Stage	2nd Stage	
System Total Pressure (bar)	40	70	70
Mean Effective H_2 Pressure Ratio (-)	2.21	1.82	8.38
ECHC Isothermal Efficiency (-)*	12.8%	9.1%	37.0%
ECHC Power Input (W)	14.5	32.1	26.8
Cooling Temperature (K)	179	99	35
Cooling Power (W)	0.22	0.20	0.20
Volume (L)	0.83	1.90	1.12
Electrical Power Input (W_e)	14.5	32.1	26.9
Total System Mass (kg)	7.2		
Total Electrical Power Input (W_e)	73.5		
Percentage of Carnot efficiency (-)	2.1%		

* For a membrane conductivity of 0.01 S/cm, a membrane thickness of 250 μm and a current density of 0.025 A/cm^2

The average pressure ratio in the first and second stages are 2.2 and 1.8, respectively, while the pressure ratio in the hydrogen J-T stage is 8.4. Consequently, the ECHC in the third stage is much more efficient than those in the first and second stages. The predicted isothermal compression efficiency for third stage ECHC is quite high, about 37%. In predicting this efficiency, it is assumed that the membrane developed in the near term will have a slightly higher performance than the proof-of-concept membrane demonstrated in this program, achieving a proton conductivity of 0.01 S/cm at 120°C. It is also assumed that the membrane thickness can be reduced to 250 μm in the near term, which is still about twice the thickness of current commercial Nafion membranes.

The predicted total power input to the cryocooler is about 73.5 W. The corresponding COP is about 2.1% of a Carnot cycle. This performance is competitive with other solid-state cryocooler technologies.

Preliminary ECHC Design. An actual ECHC will have multiple cells to increase the membrane surface area and thus the mass flow rate across the membrane. The configuration of the ECHC is very similar to a typical planar hydrogen fuel cell stack. The ECHC comprises a stack of bipolar plates with integrated flow channels alternating with MEAs (Figure 8). A bipolar plate supplies voltage to its adjacent anode and cathode on each side. The integrated flow channels on each side of a bipolar plate distribute low-pressure hydrogen over the porous anode electrode and collect the high-pressure hydrogen on the cathode. Each MEA consists of a solid proton membrane sandwiched between two porous electrodes. All the MEAs in the stack are electrically connected in series. Consequently, the total electrical current passing through the entire ECHC is the same as the current that passes through a single layer of MEA.

For the dilution stages, the total gas pressure difference across the membrane is very small, and mechanical stresses on the membranes are negligible. However, in the ECHC for the hydrogen J-T stage, the pressure differential across the membrane is quite large. To provide support for the membrane, a porous medium is added between a flow field plate and an MEA. The porous medium allows the thin MEA to be fully supported while allowing hydrogen to evenly distribute across the MEA surfaces.

Part of this waste heat from the ECHC will be absorbed by the inlet cool stream that is at the spacecraft heat sink temperature, which is substantially lower than the ECHC's operating temperature of about 400 K. The rest of the waste heat will be conducted to the outer shell and removed by a heat sink.

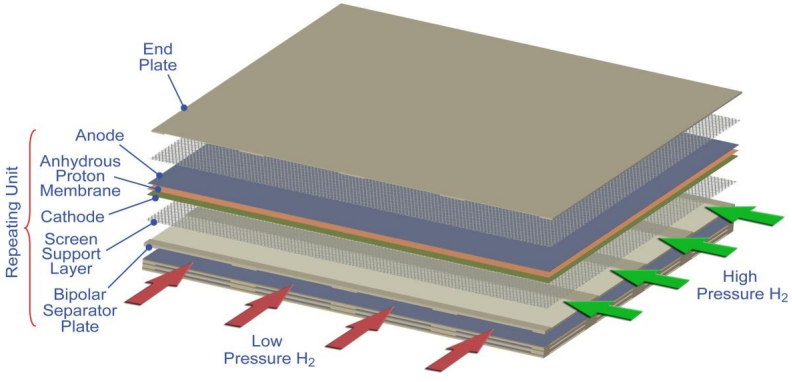

Figure 8. Simplified stack layout of an ECHC

CONCLUSION

A proof-of-concept ECHC with an anhydrous membrane was demonstrated with a compression ratio higher than 3. A unique dilution cycle was developed that enables an upper stage driven by an ECHC to use a refrigerant other than hydrogen to provide precooling for the lower hydrogen Joule-Thomson (J-T) stage. The preliminary design of a vibration-free 35 K cryocooler driven by electrochemical compressors was developed. This design study shows that the cryocooler can provide 0.2 W of cooling at 35 K at a power input of about 70 W. The cooler will have a mass of about 7.2 kg. This anhydrous proton conducting membrane technology is still in its early development stage and substantial performance improvement is quite possible. Further improvement should substantially reduce the cryocooler mass and power input. The near-term cryocooler performance will be somewhat lower than existing mechanical cryocoolers, but it will have the advantages of no moving parts, high reliability, low vibration emittance, scalability, simplicity, and low cost.

ACKNOWLEDGMENT

This research was funded by an STTR award from MDA. The guidance from AFRL at Kirtland Air Force Base is greatly appreciated.

REFERENCES

1. Narayanan, S. R., Yen, S.-P., Liu, L., and Greenbaum, S. G., "Anhydrous Proton-Conducting Polymeric Electrolytes for Fuel Cells," *J. Phys. Chem. B*, Vol. 110, 2006, pp. 3942–3948.
2. Yang, B., Manohar, A., Prakash, G. K. S., Chen, W., and Narayanan, S. R., "Anhydrous Proton Conducting Membranes based on Poly-4-vinylpyridinium Phosphate for Electrochemical Applications," *Journal of Physical Chemistry B*, Vol. 115 (49), 2011, pp. 14462–14468.